

Provided for non-commercial research and education use.
Not for reproduction, distribution or commercial use.



This article appeared in a journal published by Elsevier. The attached copy is furnished to the author for internal non-commercial research and education use, including for instruction at the authors institution and sharing with colleagues.

Other uses, including reproduction and distribution, or selling or licensing copies, or posting to personal, institutional or third party websites are prohibited.

In most cases authors are permitted to post their version of the article (e.g. in Word or Tex form) to their personal website or institutional repository. Authors requiring further information regarding Elsevier's archiving and manuscript policies are encouraged to visit:

<http://www.elsevier.com/copyright>



Contents lists available at ScienceDirect

Journal of Colloid and Interface Science

www.elsevier.com/locate/jcis



Ion specificity of the zeta potential of α -alumina, and of the adsorption of *p*-hydroxybenzoate at the α -alumina–water interface

Manash R. Das^a, Jayanta M. Borah^a, Werner Kunz^{b,*}, Barry W. Ninham^{c,*}, Sekh Mahiuddin^{a,*}

^a Materials Science Division, North-East Institute of Science & Technology, CSIR, Jorhat 785 006, Assam, India

^b Institute of Physical and Theoretical Chemistry, University of Regensburg, D-93040 Regensburg, Germany

^c Research School of Physical Sciences and Engineering, Australian National University, Canberra 0200, Australia

ARTICLE INFO

Article history:

Received 14 October 2009

Accepted 21 December 2009

Available online 28 December 2009

Keywords:

Adsorption

Alumina

DRIFT

Hofmeister effect

Ion specificity

p-Hydroxybenzoate

Surface complexation

Zeta potential

ABSTRACT

The influence of inorganic anions (NO_3^- , I^- , Br^- , Cl^- , SO_4^{2-} , and $\text{S}_2\text{O}_3^{2-}$) and of divalent cations (Ca^{2+} and Mg^{2+}) on the zeta potential and on the isoelectric point of α -alumina in aqueous medium has been studied. The effect of the anions is highly ion specific even at salt concentrations as low as 5×10^{-4} M. This unexpected finding is in line with a recent report [Böstrom et al., J. Chem. Phys. 128 (2008) 135104]. It is also in agreement with an earlier theoretical prediction [B.W. Ninham, V.V. Yaminsky, Langmuir 13 (1997) 2097]. The results are consistent with the classical Hofmeister series, except for the case of NO_3^- . Divalent anions (SO_4^{2-} and $\text{S}_2\text{O}_3^{2-}$) decrease the magnitude of the zeta potential of α -alumina in aqueous medium, more precisely; $\text{S}_2\text{O}_3^{2-}$ produced large negative zeta potential (~ -12 to -47 mV) within the pH range of the study without the isoelectric point (IEP) of α -alumina. However, the SO_4^{2-} decreased the zeta potential of α -alumina of different magnitudes (maximum ~ 25 mV at both ends of the experimental acidic and basic pH scale) with a minor shift of the IEP (~ 0.5 unit) toward lower pH. Ca^{2+} and Mg^{2+} produce zeta potentials of α -alumina roughly equal to that of neat α -alumina but slightly higher than that of Na^+ at both sides of the IEP. We have shown further that the same ion specificity or equivalently competitive ion effects occur with the adsorption density of *p*-hydroxybenzoate onto α -alumina surfaces. The sequence of anions (with common cation) for the adsorption density of *p*-hydroxybenzoate on the α -alumina surfaces follows the Hofmeister series sequence: $\text{S}_2\text{O}_3^{2-} < \text{SO}_4^{2-} < \text{Cl}^- > \text{Br}^- > \text{I}^- > \text{NO}_3^-$. The divalent cations (Ca^{2+} and Mg^{2+}) exhibit a roughly equivalent effect on the adsorption of *p*-hydroxybenzoate onto α -alumina surfaces. Using the frequency shifts of $\nu_{\text{as}}(-\text{COO}^-)$ and $\nu_{\text{s}}(-\text{COO}^-)$ in the DRIFT spectra of *p*-hydroxybenzoate after adsorption and other characteristic peaks, we have demonstrated that *p*-hydroxybenzoate forms outer-sphere complexes onto α -alumina surfaces at pH 5 and 6 and inner-sphere complexes at pH 7, 8, and 9 in the presence of 5×10^{-4} M NaCl(aq).

© 2009 Elsevier Inc. All rights reserved.

1. Introduction

An understanding of the adsorption of surface-active agents at the metal oxide– and oxy(hydroxide)–water interface in the presence of background electrolyte of variable concentrations and pH of the suspension is important for mineral processing industries, soil remediation, wetting, dispersion stability, and mineral dissolution [1–8]. With soluble natural organic matter (NOM), carboxylic and phenolic –OH groups are the two primary functionalities present that are responsible for adsorption at the mineral oxide–water interface in nature.

The adsorption of NOM onto mineral oxide surfaces is usually attributed to electrostatic and “specific” interactions [9–11]. In this context the word “specific” really means “of yet imperfectly under-

stood origin.” A possible clue to the mechanism lies in the observation that inorganic ions also adsorb along with NOM in the adsorption process [12–16]. For example, the adsorption density of NOM and other surface-active agents on metal oxide surfaces is decreased in the presence of polyvalent inorganic anions (e.g., SO_4^{2-} , PO_4^{3-}) [10,11,12–16]. By contrast, the amount of NOM adsorbed onto metal oxide surfaces increases in the presence of divalent cations (e.g., Ca^{2+} , Mg^{2+}) [9,10,17,18]. In recent studies it was demonstrated that divalent cations govern the deposition kinetics of viruses and adsorption of bacteria for different adsorbents [19,20]. Recently, Borah et al. [15] reported that divalent anions significantly inhibit the adsorption of salicylate at the α -alumina–electrolyte interface in comparison with monovalent anions, which promote adsorption.

Knowledge of the zeta potential provides an important parameter for the explanation of the adsorption mechanism of an adsorbate at the metal oxide–water interface. The isoelectric point (IEP) or point of zero charge (pzc) of the any metal oxide surfaces

* Corresponding authors. Fax: +91 376 2370011 (S. Mahiuddin).

E-mail addresses: werner.kunz@chemie.uni-regensburg.de (W. Kunz), barry.ninham@anu.edu.au (B.W. Ninham), mahirrj@yahoo.com (S. Mahiuddin).

provides information on the cleanness of a metal oxide surface. Park [21] has compiled the IEP/pzc characteristics of metal oxides. Recently, Kosmulski [22–24] has also compiled IEP/pzc data not only for metal oxides but also for mixed oxides, sparingly soluble salts, and other materials. In the literature the IEP of aluminum oxide powder was found to be in the pH range of 4–9.5, depending on the hydration, purity, and treatment of the surfaces [21–26]. Franks and Meagher [26] reported the IEP of sapphire and α -alumina determined by streaming potential and atomic force measurement. The IEPs were pH 5–6 and pH 9.4, respectively. The differences in the IEPs were attributed to the morphologies of the surfaces in the two types of alumina.

However, as we will show, our study shows strong, systematic Hofmeister effects at very low electrolyte concentrations. This is surprising. Practically all the literature on Hofmeister effects focuses on high electrolyte concentrations, typically >0.1 M [27–29], in some cases even at lower concentrations. Interestingly, ion specificity toward surfactant bilayers [30] and zeta potential of sapphire [26,31] have been reported at millimolar salt concentrations. Electrostatic, ion–solvent, and ion–ion interactions were thought to dominate specific ion effects at low electrolyte concentrations.

To put our study into the context of Hofmeister effects in general, we remark again that the systematic effects of ions on the surface properties of a metal oxide and oxy(hydroxide) in aqueous medium provide an important, unexplored probe that in principle should provide some insights into adsorption phenomena with surface-active agents. This is assumed to be so because the ions greatly alter the surface charge of a metal oxide and oxy(hydroxide). But as we shall see this cannot be the whole story.

The Hofmeister series originally referred to the relative flocculating capacity of a series of inorganic anions at fixed cation, or vice versa, and the ion specificity is demonstrated in a vast array of physicochemical and biological phenomena ranging from human physiology to biotechnology to ecology. Hofmeister effects were first identified more than a century ago. They were first discovered in studies of the precipitation of protein ovalbumin. (In his first works Hofmeister also explored the effects in precipitation of Fe_2O_3 .) The phenomena are so well reviewed that they need little recapitulation here [32,33]. We remark only that these Hofmeister or specific ion effects are as ubiquitous as they are unexplained. They occur in biochemistry, colloids, polymers, and surface chemistry [34]. Of closest relevance to our study, the Hofmeister series exhibit significant effects particularly on surface tensions of electrolytes [35] and surfactants [36], zeta potential and surface potential measurements [27–29,37], cationic microemulsions [38], on octadecyl monolayers spread on salt solution [39], and on interfacial water with cationic surfactant [40], water/macromolecule interfaces [41], and metal oxide/liquid interfaces [27–29,42–49]. Interestingly, Lyklema [50] argued that the ions at the oxide/water interface act as “potential determining” or preferably “charge determining” (e.g., H^+ , OH^- , Ag^+ , I^-). He argued that the influence of ions at the metal oxide/water interface can be interpreted in terms of “ion correlation”; however, for experimental evidence of “ion specificity” the surface charge of an adsorbent as well as the ion (salt) concentration should be high enough and that also for di- or higher valent ions. On the other hand, for realizing the ion specificity, Franks et al. [28] added “most importantly structure maker surfaces preferentially adsorbed structure maker ions and structure breaker surfaces preferentially adsorbed structure breaker ions,” which is in tune with Collins’s views [51] “small likes small and big likes big” or “soft likes soft and hard likes hard.”

But in the context of adsorption of the small organic acids (aliphatic or aromatic) at the metal oxide–water interface, the influence of the Hofmeister ion series on the adsorption of small well-defined organic acid(s) has not yet been reported in the liter-

ature. Generally, alkali salts containing anions like Cl^- , NO_3^- , ClO_4^- are used as background electrolytes for the adsorption of organic acids/anions on the metal oxide surfaces in aqueous medium. The influence of other inorganic anions (mono and divalent that occur in the common Hofmeister series) on the adsorption of small organic anions at the metal oxide–water interface seldom appears in the literature [12,13,52–54]. A competition effect between halides has recently been recognized. It accounts for the ion specificity toward hydrophobic solid surfaces at biological salt concentrations [55]. There has been little attention paid to, or awareness of, Hofmeister effects at millimolar salt concentrations, even though they do leave their footprint in decreasing or increasing the magnitude of the zeta potential of an adsorbent depending on the types of ions (cations and anions) [22,26,29,31,56]. In fact the possibility of such a low salt Hofmeister effect in zeta potential may be small, but the experimental values have already been reported [26,31] and also predicted theoretically [30,57].

The adsorption of small well-defined organic acids/anions at the metal oxide– and oxy(hydroxide)–water interface depends (classically) on the pH vis-à-vis the surface charge of an adsorbent, notably the zeta potential. Monovalent anions in the millimolar concentration range that decrease the magnitude of the zeta potential of an adsorbent without altering the isoelectric point (IEP) are termed indifferent electrolytes. An exception is iodide. For example, the IEP of rutile at 0.3 M $\text{NaI}(\text{aq})$ is reported to be at pH 6.3. It shifts further to higher pH 7.3 at 0.5 M $\text{NaI}(\text{aq})$. But for hematite at higher $\text{NaI}(\text{aq})$ concentration (say 0.4 M) the sign of the zeta potential is positive without any IEP [29]. This observation is characteristic of $\text{NaI}(\text{aq})$ as “ $\text{NaI}(\text{aq})$ is the most effective IEP shifter” [29].

But in the case of divalent anions and cations, the zeta potential of metal oxide and oxy(hydroxide) is drastically changed. The isoelectric point of anatase is shifted by around 4 units toward basic pH in the presence of 3 mM Ba^{2+} . The magnitude of the IEP shift in the presence 3 mM SO_4^{2-} is not significant. But the depression of zeta potential in the acidic pH range is worth noting. So too the trivalent anion (e.g., PO_4^{3-} phosphate) has a remarkable effect on both the IEP shift and the depression of zeta potential in the acidic pH range [23]. Therefore, the adsorption behavior of an organic anion at the metal oxide–water interface in the presence of anions and cations of 1:1 and 1:2 background electrolytes is expected to be different due to the change in surface charge of the metal oxide.

In the framework of adsorption studies, vibrational spectroscopy provides information on surface complexation of surface-active agents on metal oxide surfaces. Two of the most useful such tools for study of surface complexation between a surface-active agent and a metal oxide are diffuse reflectance infrared Fourier transform (DRIFT) and attenuated total reflection Fourier transform infrared (ATR-FTIR) spectroscopy [58–60]. For example, adsorption of benzenecarboxylate onto metal oxide surfaces occurs through the coordination of the carboxyl group with different modalities, such as monodentate, bridging, and chelating [61,62]. But the complete understanding of the mode of complexation of carboxylate on different metal oxide surfaces is still incomplete due to the complex nature of the chemical environment of the suspension. *p*-Hydroxybenzoate forms bidentate complexes with goethite surfaces through the carboxylic group and the involvement of the phenolic group in surface complexation is likely to be rare due its position (at the para position) in the benzene ring. But 2-hydroxybenzoic (salicylic acid) and 2,3-dihydroxybenzoic acids form surface complexes with metal oxide surfaces through carboxylic groups as well as phenolics [61,63]. Das and Mahiuddin [64] have also reported that *p*-hydroxybenzoate forms an outer-sphere surface complex with hematite surfaces and the phenolic group does not participate in the coordination onto hematite surfaces due to an unfavorable steric arrangement.

In the present study we have used *p*-hydroxybenzoic acid. This is a substituted benzoic acid, which is produced as a secondary metabolite by plant roots and microorganisms [65–67] for the adsorption studies. It contains both –COOH and –OH groups, which are sensitive to complexation with metal cations and surface complexation onto mineral surfaces. The adsorption profiles of *p*-hydroxybenzoic acid onto metal oxide surfaces are expected to be different in the presence of different inorganic anions and cations in an aqueous medium. The influence of a series of inorganic ions, and pH, on the adsorption of hydroxybenzenecarboxylate at the metal oxide–electrolyte interface seems an arcane preoccupation. It is not the subject of a vast literature. Therefore, we report in this paper:

- (i) The influence of different monovalent and divalent inorganic ions at 0.5 mM on the zeta potential of α -alumina.
- (ii) The kinetics of adsorption of *p*-hydroxybenzoate onto α -alumina surfaces at a fixed pH.
- (iii) Adsorption isotherms of *p*-hydroxybenzoate at the α -alumina–water interface at different pH and fixed background electrolyte.
- (iv) The influence of different monovalent and divalent ions on the adsorption of *p*-hydroxybenzoate at the α -alumina–water interface at a fixed pH; and finally.
- (v) Surface complexation of *p*-hydroxybenzoate at the α -alumina–water interface at different pH in the presence of NaCl(aq) as a background electrolyte is investigated by DRIFT spectroscopy.

2. Materials and methods

2.1. Materials

α -Alumina (>99.7%, Aldrich, Germany) was washed twice with distilled water to remove any soluble impurities, dried, and finally heated at ~ 700 °C for 3 h to remove gases and surface moisture and kept under vacuum. *p*-Hydroxybenzoic acid (>99.5%, E. Merck, India), sodium hydroxide (>99%, s.d. fine-chem, India), and hydrochloric acid (AR grade, NICE Chemicals, India) were used without further purification. *p*-Hydroxybenzoate was prepared from the reaction of *p*-hydroxybenzoic acid with sodium hydroxide solution by maintaining the solution pH at 6. The salts used, NaCl (99.5%, E. Merck), NaBr (99.5%, E. Merck), NaI (99.5%, BDH, India), NaNO₃ (99.5%, E. Merck), Na₂SO₄ (99.5%, E. Merck), Na₂S₂O₃ (99.5%, E. Merck), CaCl₂ (99.5%, E. Merck) and MgCl₂ (99.5%, E. Merck), were recrystallized from double-distilled water, dried, and kept in a vacuum desiccator. All solutions were prepared using freshly prepared double-distilled water.

2.2. Adsorbent

Differential thermal analysis (DTA) and thermogravimetric analysis (TGA), (SDT 2960, TA Corporation, USA), powder XRD (Ultima IV, Rigaku, Japan), and DRIFT (Model 2000, Perkin–Elmer, USA) spectra of dried and heated α -alumina were recorded and the results show that the alumina contains α -phase. The surface area of α -alumina was determined by the BET method and was found to be $7.29 \text{ m}^2 \text{ g}^{-1}$. The adsorption site concentration as determined by following the procedure of Hohl and Stumm [68] is estimated to be TOT ($\equiv \text{AlOH}$) = $1.815 \text{ mmol dm}^{-3}$ based on the site density of $4.54 \text{ site nm}^{-2}$.

2.3. Zeta potential

The zeta potential and the IEP of α -alumina were evaluated with the help of a Zetasizer-3000HS (Malvern Instruments, UK).

The zeta potential technique is a widely accepted standard tool of characterization of colloid science that uses electrophoresis. The interpretation of such measurements assumes the correctness of the theory of electrophoretic mobility of a particle. This is based on the classical theory of the double layer that ignores the dispersion and hydration forces that give rise to the specific ion effects studied. Consequently, while the measurements reported below are interpreted first in terms of the classical theoretical framework, it will not be a surprise if inconsistencies emerge. These inconsistencies and their ramifications will be discussed later in the text.

A suspension containing $\sim 0.005 \text{ g}$ of α -alumina in a 50 mL of double-distilled water at a fixed salt concentration was ultrasonicated with a Vibracell sonicator (VCX 500, USA) equipped with 0.5 in. Titanium horn for uniform dispersion. The pH of the suspension was initially adjusted with dilute HCl at ~ 3.0 and the zeta potential was measured with increasing pH of the suspension, obtained by adding dilute sodium hydroxide solution with the help of a multipurpose titrator (DTS 5900, Malvern, UK). The total time elapsed before the measurement started was $\sim 60 \text{ min}$. The zeta potential was measured with an uncertainty of $\pm 10\%$ at 25 °C and controlled by PCS software provided by Malvern Instruments, UK.

2.4. Adsorption kinetics

A suspension of 15 mL containing 0.5 g α -alumina, $5 \times 10^{-4} \text{ mol dm}^{-3}$ *p*-hydroxybenzoate, and $5 \times 10^{-4} \text{ mol dm}^{-3}$ NaCl solution was mixed thoroughly with the help of a vortex mixer. The suspension was equilibrated with intermittent mixing until adsorption equilibrium was judged to have been reached. The adsorption density (Γ) of *p*-hydroxybenzoate onto α -alumina (0.5 g) in a 15 mL suspension at pH 5 and $5 \times 10^{-4} \text{ mol dm}^{-3}$ NaCl(aq) was measured as a function of time at different temperatures. The suspensions at different intervals of time were cooled and centrifuged at 12,500 rpm for 15 min (relative centrifugal force = 28,790g). The residual concentration of *p*-hydroxybenzoate was estimated at $\lambda_{\text{max}} = 246 \text{ nm}$ (absorption maximum) with a UV–visible spectrophotometer, Specord 200 (Analytik Zena, Germany). The amount of *p*-hydroxybenzoate adsorbed per unit surface area of the α -alumina (adsorption density) was estimated by mass balance using the following relation:

$$\Gamma = (C_0 - C_e)V/ma, \quad (1)$$

where C_0 and C_e are the initial and residual concentration of the *p*-hydroxybenzoate in the suspension, V is the volume of the suspension, and m and a are the mass and surface area of the α -alumina, respectively.

2.5. Adsorption isotherms

The adsorption isotherms of *p*-hydroxybenzoate on the α -alumina surfaces were measured at 25 and 30 °C in a screw-capped glass tube. A suspension of 15 mL containing 0.5 g α -alumina in the presence of $5 \times 10^{-4} \text{ mol dm}^{-3}$ of NaCl(aq), NaBr(aq), NaI(aq), NaNO₃(aq), Na₂SO₄(aq), Na₂S₂O₃(aq), CaCl₂(aq), or MgCl₂(aq) was mixed thoroughly with the help of a vortex mixer. The pH of the suspension was adjusted to a desired value within ± 0.1 unit using either NaOH or HCl solution and then allowed to equilibrate for 1 h. The required amount of *p*-hydroxybenzoate was added and the pH of the suspension was readjusted, if necessary. The suspension was then allowed to equilibrate with intermittent mixing for 72 h (duration of equilibrium adsorption). After the equilibration, the suspension was then centrifuged and the residual concentration of *p*-hydroxybenzoate was estimated as outlined in the previous section.

2.6. DRIFT spectroscopy

For DRIFT spectroscopic studies 0.5 g of the α -alumina was equilibrated with 0.01 mol dm^{-3} *p*-hydroxybenzoate in the presence of $5 \times 10^{-4} \text{ mol dm}^{-3}$ NaCl(aq) at a desired pH maintained by adding either dilute NaOH(aq) or HCl(aq) solution following the same procedure adopted for adsorption. The suspension was centrifuged and the residue was washed once with distilled water, centrifuged, and dried in a vacuum desiccator over fused calcium chloride. The DRIFT spectra were recorded with a Perkin-Elmer FTIR 2000 spectrophotometer using a Perkin-Elmer DRIFT accessory (Part No. L127-5001) and Spectrum 3.2 software. In all cases spectra were recorded with 200 scanning and 4 cm^{-1} spectral resolution.

3. Results and discussion

3.1. Influence of monovalent and divalent ions on the zeta potential of α -alumina

The α -alumina used in the present studies has an IEP of 6.7 without any ions (Fig. 1). This is lowered in the presence of NaCl(aq) [5]. The present IEP of α -alumina is ~ 2.5 units lower than the reported value [21–24,26]. In general, the numerical value of the zeta potential of properly surface-hydrated alumina at pH 3 and low salt (1:1) concentration is reported to be $\sim 60 \text{ mV}$, which decreases on increasing the salt concentration. The much lower zeta potential and a low IEP are reported for sapphire [26], diaspore [69], and bayerite [70]. The reason for the low IEP of alumina particularly for sapphire is due to a lesser number of surface hydroxyl groups bound to multiple aluminum atoms. These have a low pK_a [26,71,72]. Moreover, the proton of the surface hydroxyl group is not bound strongly to the oxygen due to the poorly satisfied electronegativity of the surface hydroxyl group. Therefore, the proton is easily removed in the lower pH range. The XRD pattern of the adsorbent shows the α -alumina. For our α -alumina heat treatment and short duration aging of α -alumina suspension for $\sim 60 \text{ min}$ do not generate sufficient surface hydroxyl groups. So, the above two points contribute together for the lower IEP for the present α -alumina. Cromières et al. [73] has explained that the medium of storage also influences the IEP of α -alumina.

The variation of zeta potential of α -alumina in the presence of $5 \times 10^{-4} \text{ mol dm}^{-3}$ of NaCl(aq), NaBr(aq), NaI(aq), or NaNO₃(aq) as a function of suspension pH is also shown in Fig. 1. The IEP of α -alumina in the presence of Cl[−], Br[−], I[−], and NO₃[−] is not shifted

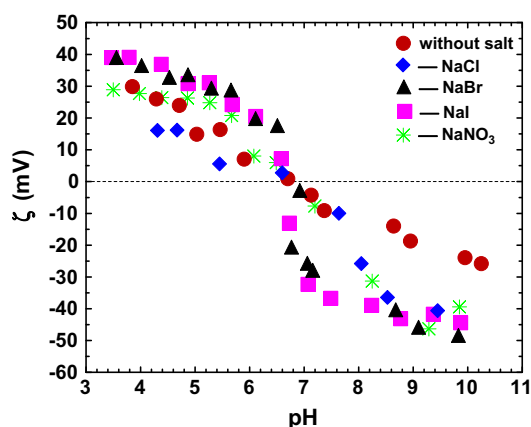


Fig. 1. Variation of zeta potential of α -alumina with pH in the presence of $5 \times 10^{-4} \text{ M}$ NaCl(aq), NaBr(aq), NaI(aq), and NaNO₃(aq) at 25 °C (initial pH of the suspension was adjusted at ~ 3.0).

or these monovalent anions are not IEP shifters at $5 \times 10^{-4} \text{ mol dm}^{-3}$. But below and above the IEP these anions exhibit their influence on the zeta potential. As an example, we consider the zeta potential of α -alumina at pH 5 and how these anions influence the zeta potential.

It is apparent from Fig. 1 that the zeta potential of α -alumina in an aqueous suspension at pH 5 without any salt can be inferred to be +22 mV. This decreases to +10 mV with Cl[−]. This is presumably due to adsorption of Cl[−] onto α -alumina surfaces resulting in a decrease in surface charge and lowering of the zeta potential. But in the presence of Br[−] and I[−] at the same concentration the zeta potential of α -alumina in the suspension increases to +33 mV. NO₃[−] increases the zeta potential of α -alumina to +25 mV but roughly equal to that of Cl[−]. It seems that Br[−], I[−], and NO₃[−] increase the surface charge of α -alumina. The influence of these monovalent anions on the zeta potential of α -alumina within the experimental uncertainties follows the sequence Cl[−] \approx NO₃[−] < Br[−] \approx I[−]. Kosmulski [29] has studied the variation of IEP α -alumina on concentration (from 1×10^{-3} to 0.5 mol dm^{-3}) of the 1:1 electrolytes and the shift of the IEP follows the sequence NO₃[−] < ClO₄[−] < Cl[−] < Br[−] < I[−]. In the presence of Br[−] and I[−] the zeta potential of α -alumina is positive in the entire pH range and no IEP was detected at concentrations $\geq 0.4 \text{ mol dm}^{-3}$ NaI(aq) and $> 0.5 \text{ mol dm}^{-3}$ NaBr(aq). The reason for this shift of IEP of α -alumina is due to the leveling off of anion adsorption at relatively higher concentrations, where the salting-in and salting-out property anion plays an important role [32,33,35]. At high salt concentration the shifting of the IEP of a metal oxide is dependent on the nature of the cation and anion. But at low background electrolyte (1:1) concentration, as in the present system, the IEP of α -alumina is independent of the nature of the 1:1 electrolyte at the millimolar concentration region. The monovalent anion binding onto α -alumina in a suspension and the effect on the zeta potential are also reported [27,28]. Johnson et al. reported an equivalent zeta potential of α -alumina in the presence of Br[−], Cl[−], I[−], and NO₃[−] at 0.01 and 1.0 M and pH 4–12 and the hydration enthalpy was the key parameter for almost identical binding properties [27]. On the other hand, Franks et al. reported binding of IO₃[−], BrO₃[−], Cl[−], NO₃[−], and ClO₄[−] onto α -alumina and these anion sequences follow the Hofmeister series based on the ion–solvent interaction [28]. Barring the results of Johnson et al. [27], the ion specificity results of Franks et al. [28], Kosmulski results [29], and our results follow the Hofmeister series according to ion–solvent interaction as well as polarizability, albeit the order may be reverse for either structure-making and -breaking ions or both. For example, the anions selected by Franks et al. [28] according to the ion–solvent interactions [28] follows the order taking Cl[−] as the reference IO₃[−] > BrO₃[−] > Cl[−] > NO₃[−] > ClO₄[−], but according to polarizability [74] the order follows IO₃[−] > BrO₃[−] > Cl[−] < NO₃[−] < ClO₄[−]. Enthalpy of hydration is related to salting-in and salting-out properties of ions vis-à-vis the binding property to metal oxide surface [27]. Adsorption/binding of anions (Cl[−], Br[−], I[−], and NO₃[−]) on the α -alumina surfaces based on the hydration enthalpies should follow the sequence Cl[−] > Br[−] > NO₃[−] \rightarrow I[−]. This sequence was not observed by Johnson et al. [27]. Rather, an equivalent binding effect of these anions was reported in the pH range 4–12 at 0.01 and 1.0 mol dm^{−3}. In our system also the hydration enthalpies of the anions in question have no sequential effect on the zeta potential of α -alumina. The lower value of the zeta potential of α -alumina in the presence of Cl[−] in comparison to Br[−], I[−], and NO₃[−] is due to the specific adsorption of the Cl[−] ion on the α -alumina surfaces [75] and the adsorption is ion specific.

On the other hand, SO₄^{2−} decreases the magnitude of the zeta potential of α -alumina from $\sim +20$ to $\sim +7 \text{ mV}$ at 0.5 mM and pH 5, whereas S₂O₃^{2−} decreases the magnitude of the zeta potential significantly from $\sim +20$ to $\sim -29 \text{ mV}$ (Fig. 2). There is a marginal shift of the IEP of α -alumina also in the presence of SO₄^{2−} which was found to be 6.2. But the zeta potential is negative in the presence

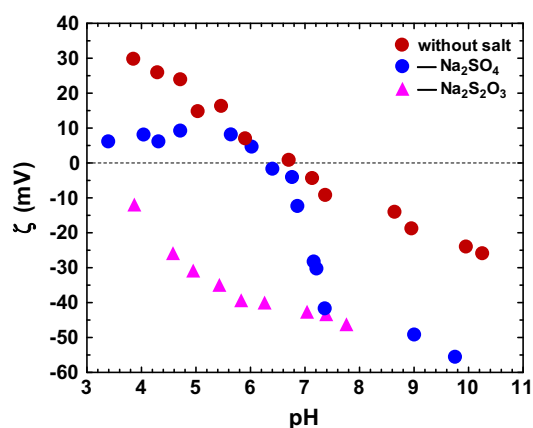


Fig. 2. Variation of zeta potential of α -alumina with pH in the presence of 5×10^{-4} M $\text{Na}_2\text{SO}_4(\text{aq})$ and $\text{Na}_2\text{S}_2\text{O}_3(\text{aq})$ at 25°C (initial pH of the suspension was adjusted at ~ 3.0).

of $\text{S}_2\text{O}_3^{2-}$ over the entire pH range and no IEP at all can be detected. The change in the magnitude of the zeta potential of α -alumina would be assigned conventionally to the specific adsorption of SO_4^{2-} and $\text{S}_2\text{O}_3^{2-}$ in the outer Helmholtz plane of the α -alumina surfaces, making the surface negatively charged [76,77].

Taking these results together at pH 5 we conclude that the structure-making ions ($\text{S}_2\text{O}_3^{2-}$ and SO_4^{2-}) decrease the magnitude of the zeta potential of α -alumina numerically more than the structure-breaking ions (NO_3^- , Br^- , and I^-) while Cl^- represents border line. Interestingly, the Hofmeister series effect for the present anions is observed and follows the order $\text{S}_2\text{O}_3^{2-} < \text{SO}_4^{2-} < \text{Cl}^- \approx \text{NO}_3^- < \text{Br}^- \approx \text{I}^-$ [32–35] with an exception for NO_3^- . The sequence is in line of their polarizability and ion–ion interaction effect. In the acidic and alkali pH range a reverse Hofmeister series effect among halides (Cl^- , Br^-) and NO_3^- was demonstrated after considering the nonelectrostatic force in the well-known DLVO theory in precipitation of oxide in suspension [78]. An exception in the form of a reverse Hofmeister series effect has also been encountered, depending on the choice of system and/or salt concentration [79].

The variation of the zeta potential of α -alumina as a function of pH in the presence of divalent cation at 5×10^{-4} mol dm^{-3} and at 25°C is shown in Fig. 3. The zeta potential of α -alumina in the presence of Ca^{2+} and Mg^{2+} is found to be +25 mV at pH 5, which is roughly comparable to that with neat α -alumina. It is apparent

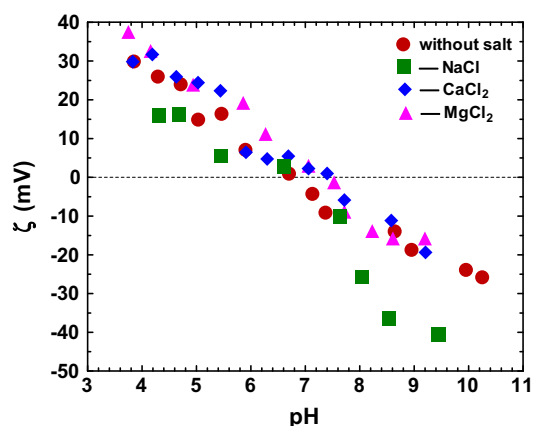


Fig. 3. Variation of zeta potential of α -alumina with pH in the presence of 5×10^{-4} M $\text{CaCl}_2(\text{aq})$ and $\text{MgCl}_2(\text{aq})$ at 25°C (initial pH of the suspension was adjusted at ~ 3.0).

that Ca^{2+} and Mg^{2+} have a less significant influence on the zeta potential of α -alumina in comparison to anions (Fig. 2). But the effect on the zeta potential is positive, taking Na^+ as the base value. On the contrary the IEP of α -alumina is shifted from 6.78 to 7.4 in the presence of Ca^{2+} and Mg^{2+} . This was not observed in the presence of monovalent anions under similar experimental conditions. The shifting of the IEP of α -alumina by divalent anions and cations in the present study is opposite in nature. Such shifting of the IEP of α -alumina is due to the adsorption of the SO_4^{2-} , Ca^{2+} , and Mg^{2+} on the α -alumina surfaces [80] and alteration of surface charge of the α -alumina surface.

With the results in hand, we conclude that the structure maker ions adsorbed preferentially onto the α -alumina surfaces (structure maker). Also the ion with higher polarizability has higher surface-active properties [30]. Even though the present α -alumina has lesser surface hydroxyl groups in contrast to reported higher surface hydroxyl groups, due to short duration aging, the ion specificity is observed for all ions (anions and cation) in the present study. Ion–solvent and ion–ion interactions and equally the polarizability of ions in the millimolar concentration region and below are the governing factors for changing the magnitude of the zeta potential of α -alumina in the suspension. Therefore, the adsorption profile of an adsorbate (in the present study it is *p*-hydroxybenzoate) onto α -alumina surfaces in the presence of these anions individually is expected to be different since there would be competition between an ion and an adsorbate for the surface site as the surface charge and the interaction at the double layer at the solid/liquid interface are ion specific [30]. This will be discussed in the next section.

3.2. Kinetics of adsorption

The variation of adsorption density of *p*-hydroxybenzoate at the α -alumina/water interface at pH 5, 5×10^{-4} mol dm^{-3} $\text{NaCl}(\text{aq})$ and at three different temperatures is shown in Fig. 4. The state of adsorption equilibrium for *p*-hydroxybenzoate at the α -alumina–water interface is attained after 70 h in the temperature range of the study. The state of adsorption equilibrium is found to be similar to that of the *p*-hydroxybenzoate–hematite system reported earlier [64]. Therefore, an equilibration time of 72 h is chosen for the adsorption isotherms.

The kinetic parameters and the rate constants for adsorption were estimated using pseudo-first-order [81,82] and pseudo-second-order kinetic equations of linear form and the Ho equation, which is the nonlinear form of pseudo-second-order kinetic equation [83–86].

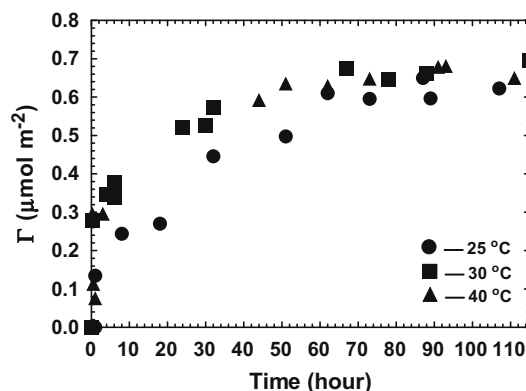


Fig. 4. Effect of temperature on the adsorption of *p*-hydroxybenzoate on α -alumina surfaces at fixed initial concentration of *p*-hydroxybenzoate: $C_0 = 5 \times 10^{-4}$ M, α -alumina = 0.5 g, $\text{NaCl}(\text{aq}) = 5 \times 10^{-4}$ M, $V = 15$ mL, pH 5.0.

$$\ln(q_e - q) = \ln q_e - k_1 t \quad (2)$$

$$t/q = 1/k_2 q_e^2 + (1/q_e)t \quad (3)$$

$$q = q_e^2 k_3 t / (k_3 q_e t + 1), \quad (4)$$

where q_e and q are the concentration of p -hydroxybenzoate adsorbed on α -alumina surfaces at equilibrium and at time t and k_1 , k_2 , and k_3 are the adsorption rate constant for the pseudo-first-order, pseudo-second-order, and the Ho kinetics equations. The estimated value of q_e from the pseudo-first-order kinetic equations deviates (up to ~90%) from the experimental q_e value. This has also been encountered for many systems and the reasons for such deviations discussed by many authors [15,64,85–89]. Regarding the pseudo-second-order kinetic equation of linear form many authors have raised the question of applicability due to associated statistical errors [85,86,89]. Both these kinetic equations of linear form are applicable to adsorption kinetics data for a system not far from the state of equilibration. In contrast, the nonlinear form of the pseudo-second-order kinetics equation, i.e., Ho equation (Eq. (4)) is applicable in the entire time duration of an adsorption kinetics run.

Estimated values of the parameters of Eqs. (2), (3), and (4) are presented in Table 1. From the standard deviations (Table 1) these imply that the calculated value of the q_e parameter obtained from the pseudo-first-order and the pseudo-second-order kinetics equations is not in good agreement (up to ~42% deviation) with that of the experimental q_e while the Ho equation exhibits better agreement.

3.3. Adsorption isotherms

The adsorption isotherms of the p -hydroxybenzoate– α -alumina system at different pHs, 5×10^{-4} mol dm $^{-3}$ NaCl(aq), and at 30 °C are shown in Fig. 5. The adsorption isotherms have a Langmuir form and the Langmuir equation of the following form was used to fit the experimental adsorption data,

$$\Gamma = \Gamma_{\max} C_e / (K + C_e), \quad (5)$$

where C_e is the equilibrium concentration of p -hydroxybenzoate (in mmol dm $^{-3}$), $K = 1/K_s$, K_s is the adsorption coefficient, and Γ and Γ_{\max} are the adsorption of the p -hydroxybenzoate (in $\mu\text{mol m}^{-2}$) at equilibrium and after saturation on the α -alumina surfaces, respectively. The values of Γ_{\max} and K_s are listed in Table 2. Tejedor-Tejedor et al. [90] has also found adsorption isotherms of the same form for the adsorption of p -hydroxybenzoate on the goethite surfaces at pH 5.5 and 20 °C. The adsorption density of p -hydroxybenzoate at the α -alumina–electrolyte interface decreases with the increase of pH of the suspension. This is due to the decrease in the positive sites at the α -alumina surface with increased pH of the suspension. As expected from the zeta potential

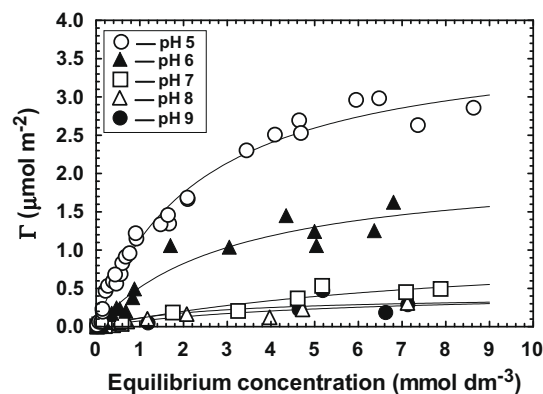


Fig. 5. Adsorption isotherms of p -hydroxybenzoate onto α -alumina surfaces at different pHs, NaCl(aq) = 5×10^{-4} M, α -alumina = 0.5 g, $V = 15$ mL, and at 30 °C. Symbols are experimental and the solid lines are the theoretical value (Eq. (5)), respectively. The data points represent triplicate adsorption experiments.

in the presence of NaCl(aq) (Fig. 1) the adsorption density of p -hydroxybenzoate onto α -alumina at IEP (pH 6.78 and above) should have been numerically zero. In contrast the experimental adsorption density at pH 7 is $\sim 1 \mu\text{mol m}^{-2}$. At pH 7 and above p -hydroxybenzoate is adsorbed onto the neutral surface site on the α -alumina, which is likely to be nonelectrostatically driven.

3.4. Influence of mono- and divalent ions on the adsorption isotherms

The influence of the anions representing the Hofmeister series and the divalent cations at a concentration of 5×10^{-4} mol dm $^{-3}$ on the adsorption isotherms at pH 5 is discussed in this section. The variation of the adsorption density of p -hydroxybenzoate on the α -alumina surfaces in the presence of Cl $^{-}$, Br $^{-}$, I $^{-}$, and NO $_3^{-}$ is shown in Fig. 6. The adsorption isotherms are of Langmuir form.

The Γ_{\max} and K_s values so obtained by using Eq. (5) are presented in Table 3. Γ_{\max} values in the presence of the monovalent anions follow the Hofmeister anion series sequence NO $_3^{-}$ < I $^{-}$ < Br $^{-}$ < Cl $^{-}$ or the ion competitive effect follows the sequence NO $_3^{-}$ > I $^{-}$ > Br $^{-}$ > Cl $^{-}$. The polarizability sequence among the halogen ions is Cl $^{-}$ < Br $^{-}$ < I $^{-}$ (Cl $^{-}$ = 3.76, Br $^{-}$ = 5.07, I $^{-}$ = 7.41 Å 3) [74]. Nevertheless, the higher the polarizability of an ion, the higher the surface-active property [36]. In that case, among the halides, I $^{-}$ is more surface active followed by Br $^{-}$ and Cl $^{-}$. Therefore, the adsorption of p -hydroxybenzoate onto α -alumina surfaces will be less (different numerical values) in the presence of halides and the sequence of Γ_{\max} is in the right direction of Hofmeister series. But this polarizability rule is not followed by NO $_3^{-}$ (4.48 Å 3) [74]. Recent work that evaluates polarizabilities of ions and their frequency dependencies from ab initio quantum mechanics shows that simple single frequency descriptions of the polarizability of

Table 1

Values of the adsorption coefficient and the rate constants for p -hydroxybenzoate adsorption on α -alumina surfaces at different temperatures and pH 5.

p -Hydroxybenzoate		25 °C	30 °C	40 °C
Pseudo-first-order kinetics	k_1 (min $^{-1}$)	0.0367	0.0408	0.0491
	q_e ($\mu\text{mol m}^{-2}$)	0.5795	0.3836	0.4802
	SD	0.0863	0.3081	0.2159
Pseudo-second-order kinetics	k_2 (min $^{-1}$ mol $^{-1}$ dm 3)	0.0743	0.2869	0.3959
	q_e ($\mu\text{mol m}^{-2}$)	0.7457	0.6892	0.6720
	SD	0.0566	0.0893	0.0974
Ho equation	k_3 (m $^2/\mu\text{mol min}$)	0.0506	0.3112	0.4264
	q_e ($\mu\text{mol m}^{-2}$)	0.7915	0.6791	0.6773
	SD	0.0446	0.0853	0.0852
Experimental	q_e ($\mu\text{mol m}^{-2}$)	0.6257	0.6620	0.6607

Table 2
Values of the Langmuir parameters as a function of pH for *p*-hydroxybenzoate adsorption on α -alumina surfaces at 30 °C.

Langmuir parameters	pH				
	5	6	7	8	9
Γ_{\max} ($\mu\text{mol m}^{-2}$)	3.819	2.114	1.093	0.4863	0.4135
K_s	0.4235	0.3193	0.1130	0.1822	0.3833
SD	0.125	0.138	0.051	0.030	0.079

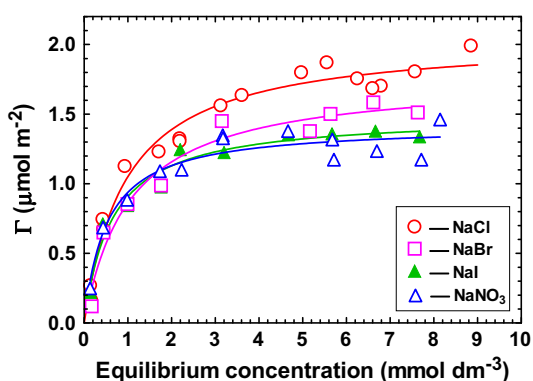


Fig. 6. Adsorption isotherm of *p*-hydroxybenzoate onto the α -alumina in the presence of 5×10^{-4} M NaCl(aq), NaBr(aq), NaI(aq), and NaNO₃(aq): α -alumina = 0.5 g, $V = 15$ mL, pH 5, and at 25 °C.

ions that determine dispersion forces of adsorption can be very misleading [91,92]. With correct polarizabilities the results seem to fall into place. NO₃⁻ is different because of its anisotropy in polarizability, which affects its adsorption.

The significant changes in adsorption density of *p*-hydroxybenzoate on the α -alumina surfaces under similar experimental conditions in the presence of the divalent anions in comparison to Cl⁻ are depicted in Fig. 7. At low initial concentration of *p*-hydroxybenzoate the adsorption density of *p*-hydroxybenzoate on α -alumina surfaces in the presence of SO₄²⁻ and S₂O₃²⁻ is quite negligible. Nevertheless, beyond a certain initial concentration of *p*-hydroxybenzoate, the adsorption density of *p*-hydroxybenzoate on α -alumina surfaces increases with the increase in concentration of *p*-hydroxybenzoate. However, no surface saturation could be observed as in the case of monovalent anions. Moreover, the adsorption density of *p*-hydroxybenzoate in the presence of divalent anions (SO₄²⁻ and S₂O₃²⁻) is lower than that of monovalent anions and it is lowest in the case of S₂O₃²⁻. Here again the polarizability of ions plays an important role; e.g., the polarizability of SO₄²⁻ is 6.33 Å³ [74] and that of S₂O₃²⁻ is 11.13 Å³ [93]. The results indicate that S₂O₃²⁻ is adsorbed more due to its higher surface-active properties [36] and follow “structure maker ions like structure maker surface” [28] that lead to lesser adsorption density of *p*-hydroxybenzoate. These experimental observations also gives an idea of competition effects between the inorganic ion and the

Table 3
Values of the Langmuir parameters for *p*-hydroxybenzoate adsorption on α -alumina surfaces with different monovalent and divalent ions at pH 5 and 25 °C in the presence of 5×10^{-4} mol dm⁻³.

Langmuir parameters	Monovalent and divalent salts							
	NaCl	NaBr	NaI	NaNO ₃	Na ₂ SO ₄	Na ₂ S ₂ O ₃	CaCl ₂	MgCl ₂
Γ_{\max} ($\mu\text{mol m}^{-2}$)	2.049	1.765	1.492	1.420	–	–	2.119	2.286
K_s	1.051	0.951	1.552	1.944	–	–	1.064	1.607
SD	0.096	0.104	0.076	0.101	–	–	0.098	0.099

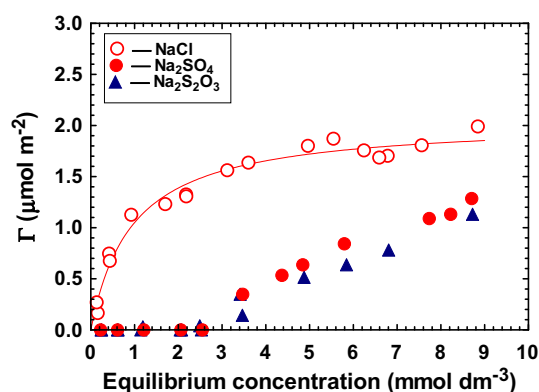


Fig. 7. Adsorption isotherm of *p*-hydroxybenzoate onto the α -alumina in the presence of 5×10^{-4} M NaCl(aq), Na₂SO₄(aq), and Na₂S₂O₃(aq): α -alumina = 0.5 g, $V = 15$ mL, pH 5, and at 25 °C.

p-hydroxybenzoate as realized for halides account for the ion specificity toward hydrophobic solid surfaces at biological salt concentrations [55].

We have already noted that the magnitude of the zeta potentials of α -alumina at pH 5 in the presence of SO₄²⁻ and S₂O₃²⁻ (+7 and –29 mV, respectively) is lower by comparison with Cl⁻ (+10 mV). Therefore, the lower magnitude of the zeta potential of α -alumina (e.g., at pH 5) in the presence of divalent anions also indicates a lower adsorption density of *p*-hydroxybenzoate on the α -alumina surfaces than in the presence of monovalent ions. The adsorption studies [12] in conjunction with the vibration spectroscopy [77] showed that SO₄²⁻ adsorbed onto aluminum oxide and goethite surfaces. Nevertheless, adsorption of SO₄²⁻ onto aluminum oxide decreases the magnitude of the zeta potential of α -alumina. These phenomena inhibit flotation of alumina due to lower adsorption of an ionic collector [56]. In the present system we also realized the ion competitive effect [55] between divalent anion (SO₄²⁻ and S₂O₃²⁻) and *p*-hydroxybenzoate for the adsorption sites of the α -alumina. At low initial concentrations (up to $C_0 \sim 2.5$ mmol dm⁻³, Fig. 7) of *p*-hydroxybenzoate, SO₄²⁻ and S₂O₃²⁻ specifically adsorb on the α -alumina surfaces. Beyond ~ 2.5 mmol dm⁻³ there exists a competition between SO₄²⁻ and S₂O₃²⁻ and *p*-hydroxybenzoate for the surface sites on α -alumina and adsorption of *p*-hydroxybenzoate begins to occur. We have not quantified how much SO₄²⁻ and S₂O₃²⁻ adsorbs on the α -alumina surfaces along with *p*-hydroxybenzoate. The order of adsorption density of *p*-hydroxybenzoate at saturation on the α -alumina surfaces in the presence of different anions representing the Hofmeister series is found to be S₂O₃²⁻ < SO₄²⁻ < Cl⁻ > Br⁻ > I⁻ > NO₃⁻. With the sole exception of NO₃⁻ the Hofmeister anions series effect is followed for the adsorption of *p*-hydroxybenzoate on α -alumina surfaces but for the halides the sequence is reverse w.r.t. zeta potential. The inversion of Hofmeister ion series is not surprising and has been observed in many systems [78,79].

The change of adsorption density of *p*-hydroxybenzoate onto α -alumina surfaces in the presence of 5×10^{-4} mol dm⁻³ Ca²⁺ and Mg²⁺ along with Na⁺ (for comparison) at pH 5 and 25 °C is

presented in Fig. 8. It is apparent from Table 3 that the maximum adsorption, Γ_{\max} , is 2.119 and 2.286 $\mu\text{mol m}^{-2}$ in the presence of Ca^{2+} and Mg^{2+} , respectively. This is numerically comparable to Na^+ but significantly higher than that of anions (Figs. 6 and 7). The higher adsorption density of *p*-hydroxybenzoate onto α -alumina in the presence of Ca^{2+} and Mg^{2+} at pH 5 than that of anions is due to the higher zeta potential of α -alumina (Fig. 3). We remark that the divalent ions (either cation or anion, Figs. 7 and 8) have a much greater effect than monovalent ions (Fig. 6) on the adsorption of *p*-hydroxybenzoate on the α -alumina surfaces under similar experimental conditions due to their higher polarizabilities. Moreover, *p*-hydroxybenzoate also possesses polarizability, but its size is higher than all inorganic ions. So, there is a competition effect between the inorganic ion and the *p*-hydroxybenzoate for the surface sites due to different polarizability and their size.

3.5. DRIFT spectra

The surface complexation of *p*-hydroxybenzoic acid onto the alumina surfaces in the presence of various ions of higher polarizability is expected to be different but here we report only the surface complexation of *p*-hydroxybenzoic acid onto the α -alumina surfaces in the presence of Cl^- . The DRIFT spectra of *p*-hydroxybenzoate (Fig. 9) exhibit peaks at 1548, 1418, and 1263 cm^{-1} (Table 4), which are assigned to $\nu_{\text{as}}(-\text{COO}^-)$, $\nu_{\text{s}}(-\text{COO}^-)$ and $\nu_{\text{C-O}}$ (between aromatic carbon and phenolic oxygen), respectively. The peak at 1611 cm^{-1} is assigned to $\nu_{\text{C-C}}$ (aromatic ring in-plane) and all peaks are in good agreement with the literature values [64,94].

The DRIFT spectra of *p*-hydroxybenzoate after adsorption on the α -alumina surfaces at pH 5, 6, 7, 8, and 9 are shown in Fig. 9 and listed in Table 4. The strong symmetric peak at 1418 cm^{-1} of the ligand on adsorption produces a band envelope at a lower frequency region. It comprises two medium peaks at 1392 and 1422 cm^{-1} at pH 5. On increasing the pH of the suspension, the symmetric band envelope shifted further to a lower frequency region and centered at $\sim 1362 \text{ cm}^{-1}$. Two weak peaks at 1422 and 1392 cm^{-1} at pH 5 and 6, respectively, are due to a C–C in-plane ring deformation [95]. The characteristic bands of $\nu_{\text{as}}(-\text{COO}^-)$ and $\nu_{\text{s}}(-\text{COO}^-)$ for the *p*-hydroxybenzoate after adsorption on the α -alumina surfaces are found at 1546 and 1392 cm^{-1} at pH 5, 1541 and 1378 cm^{-1} at pH 6, 1541 and 1362 cm^{-1} at pH 7, 1539 and 1362 cm^{-1} at pH 8, and 1539 and 1363 cm^{-1} at pH 9. The peaks at 1605, 1600, 1598, 1609, and 1595 cm^{-1} at pH 5, 6, 7, 8, and 9, respectively (Table 4), are assigned to $\nu_{\text{C-C}}$ (aromatic ring). The shifting of the peak frequency for $\nu_{\text{C-C}}$ by $\sim 2\text{--}16 \text{ cm}^{-1}$ depending on the pH of the suspension to a lower frequency region w.r.t.

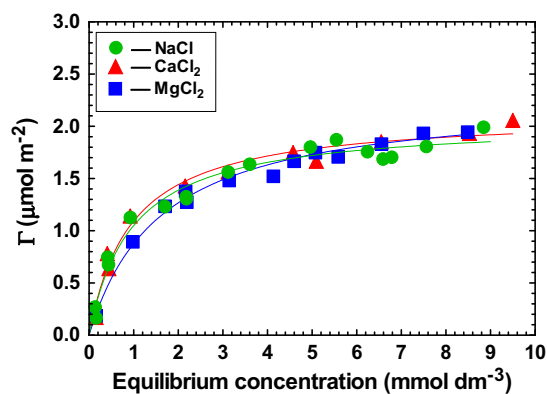


Fig. 8. Adsorption isotherm of *p*-hydroxybenzoate onto the α -alumina alumina in the presence of $5 \times 10^{-4} \text{ M}$ $\text{NaCl}(\text{aq})$, $\text{CaCl}_2(\text{aq})$, and $\text{MgCl}_2(\text{aq})$: α -alumina = 0.5 g, $V = 15 \text{ mL}$, pH 5, and at 25 $^\circ\text{C}$.

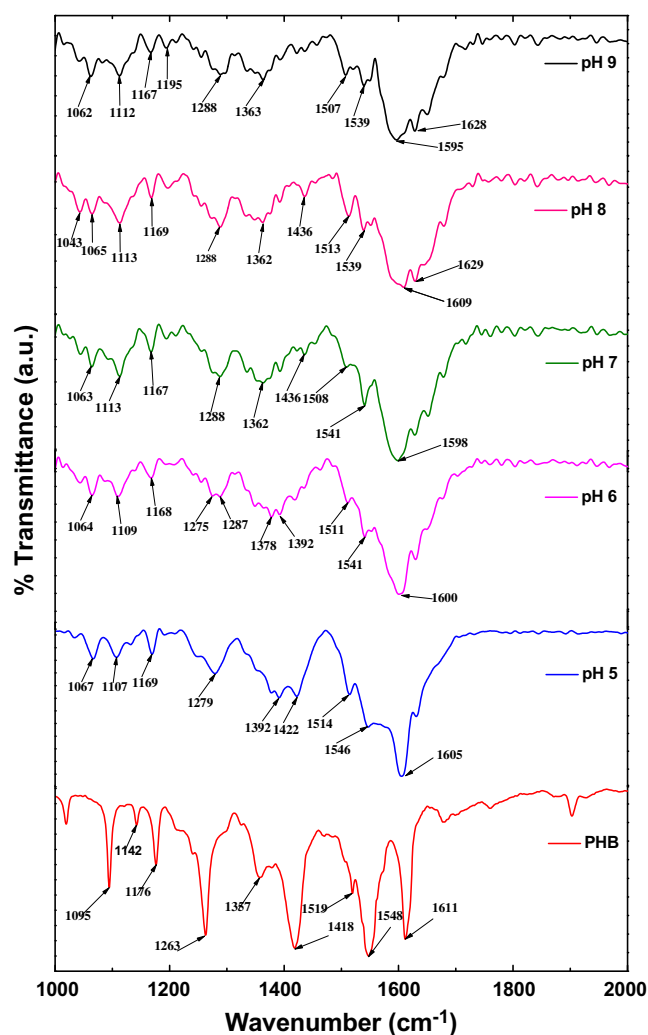


Fig. 9. DRIFT spectra of *p*-hydroxybenzoate and after adsorption on the α -alumina surfaces at different pHs and $\text{NaCl}(\text{aq}) = 5 \times 10^{-4} \text{ M}$.

Table 4

Characteristic peak frequencies of *p*-hydroxybenzoate and after adsorption on α -alumina surfaces at different pH values.

Mode	$\nu \text{ (cm}^{-1}\text{)}$					
	<i>p</i> -Hydroxybenzoate	pH 5	pH 6	pH 7	pH 8	pH 9
$\nu_{\text{s}}(-\text{COO}^-)$	1418	1392	1378	1362	1362	1363
$\nu_{\text{as}}(-\text{COO}^-)$	1548	1546	1541	1541	1539	1539
$\nu_{\text{C-C}}$ (ring)	1611	1605	1600	1598	1609	1595
$\nu_{\text{C-O}}$ ($>\text{C-OH}$)	1263	1279	1287	1288	1288	1288

1611 cm^{-1} ($\nu_{\text{C-C}}$ (aromatic ring) for the ligand) can be attributed to the change of π -electron density of *p*-hydroxybenzoate on adsorption on the α -alumina surfaces. The shift in frequency on adsorption ($\Delta\nu = \nu_{\text{as}} - \nu_{\text{s}}$ of $-\text{COO}^-$) is 154 cm^{-1} at pH 5, 154 or 163 cm^{-1} at pH 6, 179 cm^{-1} at pH 7, 177 cm^{-1} at pH 8, and 176 cm^{-1} at pH 9. These are higher than for the ionic *p*-hydroxybenzoate (130 cm^{-1} , cf., Fig. 9 and Table 4). Dobson and McQuillan [62] reported a different coordination mode of carboxylate on metal oxide surfaces. Therefore, in the present system *p*-hydroxybenzoate forms bridging complexes with the α -alumina surfaces in the aqueous medium in the presence of $\text{NaCl}(\text{aq})$. In contrast to this interpretation the use of $\Delta\nu$ as a tool for assigning surface complexation for benzene carboxylate on metal oxide surfaces has

been questioned [96]. Tejedor-Tejedor et al. [94] reported bidentate binuclear complexes of *p*-hydroxybenzoate with Fe (III) in solution, based on the shifting of the $\nu_s(-\text{COO}^-)$ band. So we are not considering the $\Delta\nu(=\nu_{\text{as}} - \nu_s \text{ of } -\text{COO}^-)$ for assigning the mode of surface complexation of *p*-hydroxybenzoate with α -alumina surface.

In the present system the phenolic $\nu_{\text{C-O}}$ appears at 1279–1288 cm^{-1} , depending on the pH. The $\nu_{\text{C-O}}$ is shifted 16 cm^{-1} at pH 5, 24 cm^{-1} at pH 6, and 25 cm^{-1} at pH 7, 8, and 9 toward the higher frequency region. Yost et al. [97] suggested that the deprotonation of phenolic oxygen is possible if the shift of $\nu_{\text{C-O}}$ is $\geq 30 \text{ cm}^{-1}$ in the higher frequency region. Moreover, Tejedor-Tejedor et al. [94] reported deprotonation of the phenolic oxygen if ν_{as} of the carboxylate is shifted by 41 cm^{-1} to a lower frequency region and also the benzene ring vibration is shifted by 21–30 cm^{-1} . In our case $\nu_{\text{as}}(-\text{COO}^-)$ is shifted only 2–9 cm^{-1} toward lower frequencies, depending on the pH. Moreover, the $\nu_{\text{C-C}}$ ring vibration is shifted only 2–16 cm^{-1} . Therefore, we can conclude that the phenolic oxygen in *p*-hydroxybenzoate is not deprotonated. The shifting of the phenolic $\nu_{\text{C-O}}$ to 25 cm^{-1} at pH 7, 8, and 9 is rather due to the loosely bound proton on the phenolic oxygen. The hydroxyl group of *p*-hydroxybenzoate does not interact with the α -alumina surfaces because of its unfavorable steric arrangement.

Further, $\nu_s(-\text{COO}^-)$ is shifted by 25–56 cm^{-1} depending on the pH of the medium and $\nu_{\text{as}}(-\text{COO}^-)$ is shifted by 2–9 cm^{-1} , which accounts for the chemisorption of *p*-hydroxybenzoate on α -alumina surfaces. We reported the chemisorption of salicylate on the α -alumina surfaces based on a similar shift of $\nu_s(-\text{COO}^-)$ toward the lower frequency region [63]. Nordin et al. [98] proposed the existence of both outer- and inner-sphere surface complexes in considering the shifts of $\nu_s(-\text{COO}^-)$ by ~ 20 and $\sim 46 \text{ cm}^{-1}$, respectively, to the high frequency region in the case of dicarboxylic acid. In the present system $\nu_s(-\text{COO}^-)$ is shifted $\sim 56 \text{ cm}^{-1}$ at pH 7, 8, and 9. This favors the inner-sphere surface complexes. But at pH 5 and 6 the shift in $\nu_s(-\text{COO}^-)$ is found to be 26 cm^{-1} , which favors the outer-sphere surface complexes. The possible surface complexes of *p*-hydroxybenzoate onto α -alumina surfaces are shown in Fig. 10.

4. Summary

The zeta potential of α -alumina is strongly affected by the addition of salts, even at very low salt concentrations. This effect is highly ion specific and, with the exception of nitrate, follows a Hof-

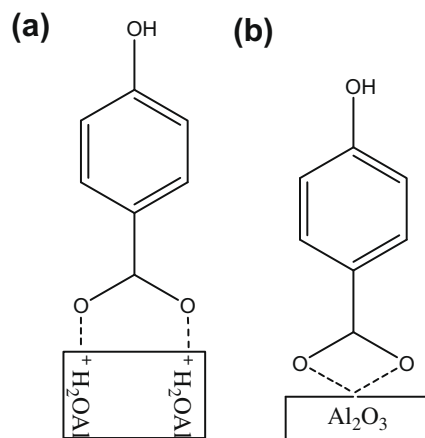


Fig. 10. Probable surface complexation of *p*-hydroxybenzoate onto α -alumina surfaces (a) outer-sphere and (b) inner-sphere.

meister series at the alumina–electrolyte interface. A similar Hofmeister effect was also detected in the surfactant (cationic) adsorption at the solution–vapor interface at $\sim 0.01 \text{ mol dm}^{-3}$ [36]. It is surprising to find the Hofmeister effect at very low electrolyte concentration ($5 \times 10^{-4} \text{ mol dm}^{-3}$) and this supports the theoretical findings [30]. We presume that at a very low electrolyte concentration the polarizability of the ions in addition to the ion–solvent and ion–ion interactions plays an important role for the Hofmeister effect in determining specific ion adsorption onto α -alumina. As a result, the adsorption of organic matter on α -alumina may also be influenced by the presence of background salt. This has been demonstrated here and studied in detail for *p*-hydroxybenzoate as a model compound. Indeed its adsorption depends on the specific added electrolyte. An ion competitive effect in adsorption occurs, as seen from the adsorption of *p*-hydroxybenzoate onto α -alumina in the presence of $\text{Na}_2\text{SO}_4(\text{aq})$ and $\text{Na}_2\text{S}_2\text{O}_3(\text{aq})$. Further, divalent cations increase the adsorption density of *p*-hydroxybenzoate. The characteristic shifting of $\nu_s(-\text{COO}^-)$ and of $\nu_{\text{as}}(-\text{COO}^-)$ suggests that outer-sphere complexes are formed at pH 5 and 6 and inner-sphere complexes at pH 7, 8, and 9. For a better understanding of the surface complexation-cum-orientation of *p*-hydroxybenzoate, surface-selective spectroscopic techniques could deliver additional information [95,99].

Acknowledgments

The authors thank the anonymous reviewer for several valuable suggestions, which were of immense help in improving the manuscript. The authors (MRD, JMD, SM) are grateful to the Department of Science & Technology the Council of Scientific & Industrial Research, New Delhi, India, for financial support and the Director, North-East Institute of Science and Technology, CSIR, Jorhat, India, for the interest in this work and facilities. The authors are thankful to Dr. D. Parson of Australian National University, Australia, for calculating the polarizability of $\text{S}_2\text{O}_3^{2-}$ and to Mr. P. Khound of NEIST, Jorhat, India, for recording the DRIFT spectra.

References

- [1] S. Subramaniam, K.A. Natarajan, Miner. Eng. 4 (1991) 587.
- [2] J.S. Laskowski, R.J. Pugh, in: J.S. Laskowski, J. Ralston (Eds.), Colloid Chemistry in Mineral Processing, Elsevier, Amsterdam, 1992 (Chapter 4).
- [3] R.F. Conkley, Practical Dispersion: A Guide to Understanding and Formulating Slurries, Wiley, VCH, New York, 1996 (Chapter II).
- [4] S.B. Johnson, T.H. Yoon, B.D. Kocar, G.E. Brown Jr., Langmuir 20 (2004) 4996.
- [5] M.R. Das, D. Bordoloi, P.C. Borthakur, S. Mahiuddin, Colloids Surf., A 254 (2005) 49.
- [6] N.I. Ivanova, I.L. Volchkova, E.D. Shchukin, Colloids Surf., A 101 (2003) 239.
- [7] S.B. Johnson, T.H. Yoon, G.E. Brown Jr., Langmuir 21 (2005) 2811.
- [8] T.H. Yoon, S.B. Johnson, G.E. Brown Jr., Langmuir 21 (2005) 5002.
- [9] E. Tipping, Chem. Geol. 33 (1981) 81.
- [10] J.A. Davis, Geochim. Cosmochim. Acta 46 (1982) 2381.
- [11] B. Gu, J. Schmitt, Z. Chen, L. Liang, J.F. McCarthy, Environ. Sci. Technol. 28 (1994) 38.
- [12] M.A. Ali, D.A. Dzombak, Environ. Sci. Technol. 30 (1996) 1061.
- [13] M.A. Ali, D.A. Dzombak, Geochim. Cosmochim. Acta 60 (1996) 5045.
- [14] K. Axe, M. Vejgård, P. Person, J. Colloid Interface Sci. 294 (2006) 31.
- [15] J.M. Borah, M.R. Das, S. Mahiuddin, J. Colloid Interface Sci. 316 (2007) 260.
- [16] R. Rahnemaie, T. Hiemstra, W.H. van Riemsdijk, J. Colloid Interface Sci. 315 (2007) 415.
- [17] E. Tipping, Geochim. Cosmochim. Acta 45 (1981) 191.
- [18] H.M. Sibanda, S.D. Young, J. Soil. Sci. 37 (1986) 197.
- [19] N. Bhosle, P.A. Suci, A.M. Baty, R.M. Weiner, G.G. Geesey, J. Colloid Interface Sci. 205 (1998) 89.
- [20] M. Pham, E.A. Mintz, T.H. Nguyen, J. Colloid Interface Sci. 338 (2009) 1.
- [21] G.A. Park, Chem. Rev. 65 (1965) 177.
- [22] M. Kosmulski, J. Colloid Interface Sci. 253 (2002) 77.
- [23] M. Kosmulski, J. Colloid Interface Sci. 275 (2004) 214.
- [24] M. Kosmulski, J. Colloid Interface Sci. 298 (2006) 730.
- [25] S. Dessel, O. Spalla, P. Lixon, B. Cabane, Colloids Surf., A 196 (2002) 1.
- [26] G.V. Franks, L. Meagher, Colloids Surf., A 214 (2003) 99.
- [27] S.B. Johnson, P.J. Scales, T.W. Healy, Langmuir 15 (1999) 2836.
- [28] G.V. Franks, S.B. Johnson, P.J. Scales, T.W. Healy, Langmuir 15 (1999) 4411.
- [29] M. Kosmulski, Langmuir 18 (2002) 785.

- [30] M. Boström, E.R.A. Lima, F.W. Tavares, B.W. Ninham, *J. Chem. Phys.* 128 (2008) 135104.
- [31] R.J. Kershner, J.W. Bullard, M.J. Cima, *Langmuir* 20 (2004) 4101.
- [32] F. Hofmeister, *Arch. Exp. Pathol. Pharmacol.* 24 (1888) 247.
- [33] W. Kunz, J. Henle, B.W. Ninham, *Curr. Opin. Colloid Interface Sci.* 9 (2004) 19.
- [34] W. Kunz, P. Nostro, B.W. Ninham, *Curr. Opin. Colloid Interface Sci.* 9 (2004) 1.
- [35] W. Kunz, L. Belloni, O. Bernard, B.W. Ninham, *J. Phys. Chem. B* 108 (2004) 2398.
- [36] G. Para, E. Jarek, P. Warszynski, *Adv. Colloids Interface Sci.* 122 (2006) 39.
- [37] R. Maheshwari, K.J. Screeram, A. Dhathathreyan, *Chem. Phys. Lett.* 375 (2003) 157.
- [38] M.C. Gurao, S.-M. Lim, E.T. Castellana, F. Albertorio, S. Kataoka, P.S. Cremer, *J. Am. Chem. Soc.* 126 (2004) 10522.
- [39] S. Murgia, M. Monduzzi, B.W. Ninham, *Curr. Opin. Colloid Interface Sci.* 9 (2004) 102.
- [40] S. Murgia, F. Portensanai, B.W. Ninham, M. Monduzzi, *Chem. Eur. J.* 12 (2006) 7889.
- [41] X. Chen, Y. Tinglu, S. Kataoka, S. Paul, *J. Am. Chem. Soc.* 129 (2007) 12272.
- [42] Th.F. Tadros, J. Lyklema, *J. Electroanal. Chem.* 17 (1968) 267.
- [43] Y.G. Bérubé, P.L. de Bruyn, *J. Colloid Interface Sci.* 28 (1968) 92.
- [44] W. Stumm, C.P. Huang, S.R. Jenkins, *Croat. Chem. Acta* 42 (1970) 223.
- [45] A. Breeuwisma, J. Lyklema, *Discuss. Faraday Soc.* 52 (1971) 324.
- [46] R. Sprycha, *J. Colloid Interface Sci.* 127 (1989) 1.
- [47] F. Dumont, J. Warlus, A. Watillon, *J. Colloid Interface Sci.* 138 (1990) 543.
- [48] M. Colic, G.V. Franks, M.L. Fisher, F.F. Lange, *Langmuir* 13 (1997) 3129.
- [49] M. Colic, M.L. Fisher, *Chem. Phys. Lett.* 291 (1998) 24.
- [50] J. Lyklema, *Chem. Phys. Lett.* 467 (2009) 217.
- [51] K.D. Collins, *Methods* 34 (2004) 300.
- [52] M. Szekeres, E. Tombacz, K. Ferencz, I. Dekany, *Colloid Surf., A* 141 (1998) 319.
- [53] A.K. Bajpai, R. Sachdeva, *J. Appl. Polym. Sci.* 78 (2000) 1656.
- [54] W. Bouguerra, M.B.S. Ali, B. Homrouni, M. Dhahbi, *Desalination* 206 (2007) 141.
- [55] E.R.A. Lima, M. Boström, D. Horinek, E.C. Biscaia Jr., W. Kunz, F.W. Tavares, *Langmuir* 24 (2008) 3944.
- [56] D.W. Fuerstenau, Prodig, *Adv. Colloid Interface Sci.* 114–115 (2005) 9.
- [57] B.W. Ninham, V.V. Yaminsky, *Langmuir* 13 (1997) 2097.
- [58] A.R. Hind, S.K. Bhargava, A. McKinnon, *Adv. Colloid Interface Sci.* 93 (2001) 91.
- [59] O. Francioso, S. Sánchez-Cortés, V. Tugnoli, C. Marzadori, C. Ciavatta, *J. Mol. Struct.* 565–566 (2002) 481.
- [60] S. Kang, B. Xing, *Langmuir* 23 (2007) 7024 (and references therein).
- [61] M.V. Biber, W. Stumm, *Environ. Sci. Technol.* 28 (1994) 763.
- [62] K.D. Dobson, J. McQuillan, *Spectrochim. Acta, Part A* 56 (2000) 557.
- [63] M.R. Das, O.P. Sahu, P.C. Borthakur, S. Mahiuddin, *Colloids Surf., A* 237 (2004) 23.
- [64] M.R. Das, S. Mahiuddin, *J. Colloid Interface Sci.* 306 (2007) 205.
- [65] J.M. Lynch, *CRC Crit. Rev. Microbiol.* 5 (1976) 67.
- [66] G.P. Sparling, D. Vaughan, *J. Sci. Food Agric.* 32 (1981) 625.
- [67] U. Blum, *J. Nematol.* 28 (1996) 259.
- [68] H. Hohl, W. Stumm, *J. Colloid Interface Sci.* 55 (1976) 281.
- [69] W.Q. Qin, Y.H. Hu, G.Z. Qiu, H. Jiang, *Trans. Nonferr. Metal. Soc. China* 11 (2001) 430.
- [70] K. Pulfer, P.W. Schindler, J.C. Westall, R. Grauer, *J. Colloid Interface Sci.* 101 (1984) 554.
- [71] H. Knozinger, P. Ratnasamy, *Catal. Rev. Sci. Eng.* 17 (1978) 31.
- [72] C. Contescu, J. Jagiello, J.A. Schwarz, *Langmuir* 9 (1993) 1754.
- [73] L. Cromières, V. Moulin, B. Fourest, E. Giffaut, *Colloids Surf., A* 202 (2002) 101.
- [74] N.C. Pyper, C.G. Pike, P.P. Edwards, *Mol. Phys.* 76 (1992) 353.
- [75] E. Tombác, Z. Libor, E. Illés, A. Majzik, E. Klumpp, *Org. Geochem.* 35 (2004) 257.
- [76] R.J. Hunter, *Zeta Potential in Colloid Science*, Academic Press, London, 1981.
- [77] H. Wijnja, C.P. Schulthess, *J. Colloid Interface Sci.* 229 (2000) 286.
- [78] M. Boström, V. Deniz, G.V. Franks, B.W. Ninham, *Adv. Colloid Interface Sci.* 123–126 (2006) 5.
- [79] Y. Zhang, P.S. Creamer, *Proc. Natl. Acad. Sci.* 106 (2009) 15249.
- [80] C.P. Huang, W. Stumm, *J. Colloid Interface Sci.* 43 (1973) 409.
- [81] S. Lagergren, K. Svenska, V.K. Handlingar, *Kungliga Svenska Vetenskapsakademiens* 24 (1898) 1.
- [82] Y.S. Ho, *Scientometrics* 59 (2004) 171.
- [83] Y.S. Ho, G. Mckay, *Chem. Eng. J.* 70 (1998) 115.
- [84] Y.S. Ho, G. Mckay, *Process Biochem.* 34 (1999) 451.
- [85] Y.S. Ho, *Water Res.* 40 (2006) 119.
- [86] Y.S. Ho, *J. Hazard. Mater.* 136 (2006) 681.
- [87] Y. Chen, S. Liu, G. Wang, *J. Colloid Interface Sci.* 303 (2006) 380.
- [88] S. Sengupta, K.G. Bhattacharyya, *J. Colloid Interface Sci.* 295 (2006) 21.
- [89] K.V. Kumar, *J. Hazard. Mater.* 142 (2007) 564.
- [90] M.I. Tejedor-Tejedor, E.C. Yost, M.A. Anderson, *Langmuir* 8 (1992) 525.
- [91] A. Salis, D.F. Parsons, M. Boström, L. Medda, B. Barse, B.W. Ninham, M. Monduzzi, *Langmuir*, in press. doi:10.1021/la902721a.
- [92] D.F. Parsons, B.W. Ninham, *Langmuir*, in press. doi:10.1021/la902533x.
- [93] D. F. Parson, 2009 Private communication.
- [94] M.I. Tejedor-Tejedor, E.C. Yost, M.A. Anderson, *Langmuir* 6 (1990) 979.
- [95] X. Hou, Y. Fang, *J. Colloid Interface Sci.* 316 (2007) 19.
- [96] N. Nilsson, P. Persson, L. Lövgren, S. Sjöberg, *Geochim. Cosmochim. Acta* 60 (1996) 4385.
- [97] E.C. Yost, M.I. Tejedor-Tejedor, M.A. Anderson, *Environ. Sci. Technol.* 24 (1990) 822.
- [98] J. Nordin, P. Persson, E. Laiti, S. Sjöberg, *Langmuir* 13 (1997) 4085.
- [99] F. Vidal, A. Tadjeddine, *Rep. Prog. Phys.* 68 (2005) 1095.